

3 Isogeometric finite elements in nonlinear elasticity

As a first step towards nonlinear frequency analysis, we now apply the isogeometric finite element method, which we have already introduced in preceding Chapter 2, for the spatial semi-discretization of nonlinear continuum mechanics and dynamics.

First, we give a basic introduction to the 3-dimensional continuum mechanics background, i.e. kinematics, constitutive laws for hyperelasticity and visco-hyperelasticity, and governing partial differential equations in Section 3.1. Then we apply the isogeometric finite element discretization to nonlinear elasticity, present solution methods for the arising nonlinear equation system of elastostatics and review its properties in Section 3.2. Furthermore, we include brief descriptions of linear elasticity (Section 3.3) and of the nonlinear Euler-Bernoulli beam model (Section 3.4), since these problems are also relevant for feasibility, validation and benchmarking of nonlinear methods. Finally, in Section 3.5, we use computational examples to demonstrate the properties of the isogeometric approach and validate the implementations.

3.1 Continuum mechanics introduction

An introduction into continuum mechanics is given based on the monographs [20, 35, 83, 130]. The focus lies on ingredients necessary for the (isogeometric) finite element formulation of nonlinear elasticity, which is then introduced in Section 3.2.

3.1.1 Kinematics

Motion and deformation of a solid body over time can be described with respect to its *initial* or *reference configuration* given by the domain $\bar{\Omega}$, the closure of an open, bounded and connected set $\Omega \in \mathbb{R}^3$. At every time $t \in \mathbb{R}^+$, the *current* position $\mathbf{y} \in \Omega_t \subset \mathbb{R}^3$ of each *material* point $\mathbf{x} \in \Omega$ can be expressed in terms of its initial position and a *displacement* vector field $\mathbf{u} : \Omega \times \mathbb{R}^+ \rightarrow \mathbb{R}^3$ (see also Figure 3.1):

$$\mathbf{y}(\mathbf{x}, t) = \mathbf{x} + \mathbf{u}(\mathbf{x}, t). \quad (3.1)$$

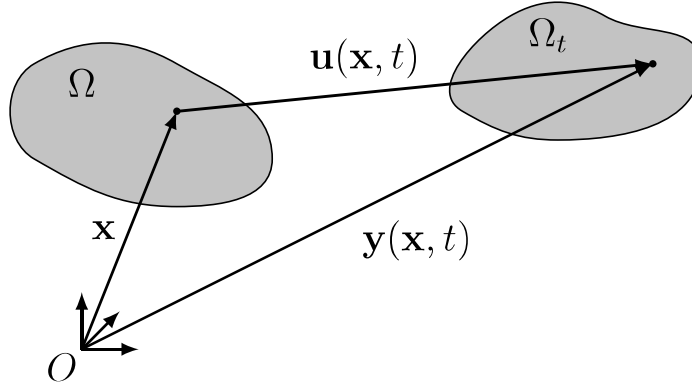


Figure 3.1: Motion of a solid body with domain Ω . At time t the current position \mathbf{y} of a material point is given in terms of its initial position \mathbf{x} and displacement \mathbf{u}

The term *Lagrangian configuration* is used when deformation is described with respect to the initial, reference or material coordinates \mathbf{x} . It is also possible to use the *Eulerian description*, where deformation is expressed with respect to the current or spatial coordinates \mathbf{y} . In the following all kinematic and other quantities are only referring to the Lagrangian configuration.

Deformation gradient

For the description of the deformation process we need a tensor, which maps material line elements $d\mathbf{x}$ onto spatial line elements $d\mathbf{y}$:

$$d\mathbf{y} = \mathbf{F} d\mathbf{x}. \quad (3.2)$$

This *deformation gradient* $\mathbf{F} : \Omega \times \mathbb{R}^+ \rightarrow \mathbb{R}^{3 \times 3}$ can be expressed as the gradient of current position with respect to initial position of each material point:

$$\mathbf{F}(\mathbf{x}, t) = \frac{d\mathbf{y}}{d\mathbf{x}}(\mathbf{x}, t) = \mathbf{I} + \frac{d\mathbf{u}}{d\mathbf{x}}(\mathbf{x}, t) = \mathbf{I} + \nabla \mathbf{u}(\mathbf{x}, t). \quad (3.3)$$

Since the mapping in (3.2) must be bijective and self-penetration of the body is excluded, the Jacobian determinant $J = \det \mathbf{F}$ must not be singular and $J > 0$. J is a measure of the volume change of the body and for incompressible materials, which are addressed separately in Chapter 6, it must hold $J \equiv 1$.

Strain measures

Furthermore we need strain measures defined in the initial configuration, such as the *Green-Lagrange strain tensor*:

$$\mathbf{E}(\mathbf{x}, t) = \frac{1}{2}(\mathbf{C}(\mathbf{x}, t) - \mathbf{I}). \quad (3.4)$$

It is defined using the *right Cauchy-Green tensor*

$$\mathbf{C}(\mathbf{x}, t) = \mathbf{F}^T \mathbf{F} = \mathbf{I} + \nabla \mathbf{u}^T + \nabla \mathbf{u} + \nabla \mathbf{u}^T \nabla \mathbf{u}, \quad (3.5)$$

which is a quadratic expression in terms of the deformation gradient \mathbf{F} resp. the displacement gradient $\nabla \mathbf{u}$.

Time derivatives

For time-dependent problems and in the case of history resp. time-dependent constitutive laws the time-derivatives of kinematic quantities also need to be considered. The velocity and acceleration of a material point in the reference configuration read as:

$$\begin{aligned}\mathbf{v}(\mathbf{x}, t) &= \frac{d\mathbf{y}}{dt} = \dot{\mathbf{y}}(\mathbf{x}, t) = \dot{\mathbf{u}}(\mathbf{x}, t), \\ \mathbf{a}(\mathbf{x}, t) &= \frac{d^2\mathbf{y}}{dt^2} = \ddot{\mathbf{y}}(\mathbf{x}, t) = \ddot{\mathbf{u}}(\mathbf{x}, t).\end{aligned}\tag{3.6}$$

The time-derivative of the deformation gradient is

$$\dot{\mathbf{F}}(\mathbf{x}, t) = \nabla \dot{\mathbf{u}} = \nabla \mathbf{v},\tag{3.7}$$

and of the Green-Lagrange and Cauchy-Green strain tensor it is

$$\dot{\mathbf{E}}(\mathbf{x}, t) = \frac{1}{2}\dot{\mathbf{C}}(\mathbf{x}, t) = \frac{1}{2}\left(\mathbf{F}^T \dot{\mathbf{F}} + \dot{\mathbf{F}}^T \mathbf{F}\right).\tag{3.8}$$

3.1.2 Balance equations

With the kinematic quantities introduced in the preceding Section 3.1.1, we can follow [20, 130] in formulating the strong form of local balance differential equations in the Lagrangian configuration. These must hold for all material points $\mathbf{x} \in \Omega$ at times $t \in \mathbb{R}^+$.

ρ_0 being the initial and ρ the current mass density of the object, the *conservation of mass* reads as

$$\int_{\Omega_t} \rho(\mathbf{y}, t) d\mathbf{y} = \int_{\Omega} \rho_0(\mathbf{x}) d\mathbf{x},\tag{3.9}$$

which can be simplified to:

$$\rho J = \rho_0.\tag{3.10}$$

From the *conservation of linear momentum* the main partial differential equation describing motion of a body subject to volume forces $\rho_0 \mathbf{b}$ is derived, *Cauchy's equation of motion*:

$$\operatorname{div} \mathbf{F} \mathbf{S} + \rho_0 \mathbf{b} = \rho_0 \ddot{\mathbf{u}}.\tag{3.11}$$

Local *balance of angular momentum* yields the symmetry of the second Piola-Kirchhoff (PK2) stress tensor

$$\mathbf{S} = \mathbf{S}^T,\tag{3.12}$$

and the *first law of thermodynamics*, i.e. conservation of energy, reads:

$$\rho_0 \dot{u} = \mathbf{S} \cdot \dot{\mathbf{E}} - \operatorname{div} \mathbf{Q} + \rho_0 R,\tag{3.13}$$

where u is the specific internal energy, R the heat source and \mathbf{Q} heat flux.

In addition to these equilibrium equations we need *boundary conditions* for displacements and tractions for the elastostatic problem:

$$\begin{aligned} \mathbf{u} &= \mathbf{h} \text{ on } \Gamma_u, \\ \mathbf{F} \mathbf{S} \mathbf{n} &= \mathbf{t} \text{ on } \Gamma_n, \end{aligned} \quad (3.14)$$

where $\Gamma_u, \Gamma_n \subset \partial\Omega$ are the parts of the boundary of the domain Ω where prescribed displacements \mathbf{h} and \mathbf{t} tractions act, and \mathbf{n} is the outer surface normal of a boundary point.

Furthermore, for time-dependent elastodynamic problems also *initial conditions* for displacements \mathbf{u} and velocities \mathbf{v} are needed:

$$\mathbf{u}(\mathbf{x}, 0) = \hat{\mathbf{u}}, \quad \mathbf{v}(\mathbf{x}, 0) = \hat{\mathbf{v}} \quad \forall \mathbf{x} \in \Omega. \quad (3.15)$$

3.1.3 Hyperelastic constitutive laws

The local balance equations as introduced in Section 3.1.2 feature a stress measure, namely the *second Piola-Kirchhoff stress tensor* \mathbf{S} , which is also defined in the material configuration. It is related to the true Cauchy stress $\boldsymbol{\sigma}$ in the current configuration by the following equation:

$$\mathbf{S} = J \mathbf{F}^{-1} \boldsymbol{\sigma} \mathbf{F}^{-T}. \quad (3.16)$$

For many materials, such as steel, aluminum or rubber, the assumption of Green elasticity or *hyperelasticity* is valid, which means that the constitutive relation of strain and stress is defined by a potential ψ , the so-called *strain energy function*. We only deal with *isotropic* materials, which means that the response of the material is indifferent from the directions. The 2nd Piola-Kirchhoff stress can then be expressed as derivative of the strain energy function w.r.t. the Green-Lagrange or right Cauchy-Green strain tensors:

$$\mathbf{S} = \frac{d\psi}{d\mathbf{E}} = 2 \frac{d\psi}{d\mathbf{C}}. \quad (3.17)$$

General hyperelastic materials

For isotropic materials it is possible to express the strain energy function in a very general way in terms of the invariants of the Cauchy-Green tensor:

$$\psi(\mathbf{C}) = \psi(I_C, II_C, III_C), \quad (3.18)$$

where the invariants can be expressed of the principal stretches, i.e. the roots λ_1, λ_2 and λ_3 of the eigenvalues of \mathbf{C} (\mathbf{C} is symmetric positive-definite):

$$\begin{aligned} I_C &= \lambda_1^2 + \lambda_2^2 + \lambda_3^2 = \text{tr}(\mathbf{C}), \\ II_C &= \lambda_1^2 \lambda_2^2 + \lambda_2^2 \lambda_3^2 + \lambda_3^2 \lambda_1^2 = \frac{1}{2} \left(\text{tr}(\mathbf{C})^2 - \text{tr}(\mathbf{C}^2) \right), \\ III_C &= \lambda_1^2 \lambda_2^2 \lambda_3^2 = \det \mathbf{C}. \end{aligned} \quad (3.19)$$

Then it follows for the 2nd Piola-Kirchhoff stress:

$$\mathbf{S} = 2 \left[\left(\frac{\partial \psi}{\partial I_C} + I_C \frac{\partial \psi}{\partial II_C} \right) \mathbf{I} - \frac{\partial \psi}{\partial II_C} \mathbf{C} + III_C \frac{\partial \psi}{\partial III_C} \mathbf{C}^{-1} \right]. \quad (3.20)$$

Since the choice of ψ is still arbitrary and material parameters have to be fitted by experiments, in practice a few choices of strain-energy functions are commonly used, including Mooney-Rivlin, Ogden and Neo-Hookean laws [130].

Material laws used in this thesis

In this work we utilize two commonly used choices of isotropic strain energy functions. The first is the linear *St. Venant-Kirchhoff* material law, which is also used in linear elasticity and restricted to large displacements and finite rotations but small strains:

$$\begin{aligned} \psi(\mathbf{E}) &= \frac{\lambda}{2} \text{tr}(\mathbf{E})^2 + \mu \text{tr}(\mathbf{E}^2), \\ \mathbf{S} &= \lambda \text{tr}(\mathbf{E}) \mathbf{I} + 2\mu \mathbf{E}, \end{aligned} \quad (3.21)$$

The second is a particular choice of a nonlinear *Neo-Hookean* material law:

$$\begin{aligned} \psi(\mathbf{C}) &= \frac{\lambda}{2} (\ln J)^2 - \mu \ln J + \frac{\mu}{2} (\text{tr}(\mathbf{C}) - 3), \\ \mathbf{S} &= \lambda \ln J \mathbf{C}^{-1} + \mu (\mathbf{I} - \mathbf{C}^{-1}). \end{aligned} \quad (3.22)$$

Both material laws include two constitutive parameters, the so-called *Lamé constants* λ and μ , which can be computed from the modulus of elasticity E (Young's modulus) and Poisson's ratio ν :

$$\lambda = \frac{\nu E}{(1 + \nu)(1 - 2\nu)}, \quad \mu = \frac{E}{2(1 + \nu)}. \quad (3.23)$$

The case of $\nu \rightarrow 0.5$ and $\lambda \rightarrow \infty$, i.e. (almost) incompressible material behavior, is addressed in Chapter 6.

Linearization

For linearization within the later described solution process the incremental constitutive 4th order tensor, or *elasticity tensor* is needed:

$$\mathbb{C} = \frac{d\mathbf{S}}{d\mathbf{E}} = \frac{d^2\psi}{d\mathbf{E}^2} = 2 \frac{d\mathbf{S}}{d\mathbf{C}} = 4 \frac{d^2\psi}{d\mathbf{C}^2} \quad (3.24)$$

For the St. Venant-Kirchhoff material it is

$$\mathbb{C}_{ijkl} = \lambda \delta_{ij} \delta_{kl} + \mu (\delta_{ik} \delta_{jl} + \delta_{il} \delta_{kj}), \quad i, j, k, l = 1, 2, 3, \quad (3.25)$$

and for the Neo-Hookean material

$$\mathbb{C}_{ijkl} = \lambda \mathbf{C}_{ij}^{-1} \mathbf{C}_{kl}^{-1} + (\mu - \lambda \ln J) (\mathbf{C}_{ik}^{-1} \mathbf{C}_{jl}^{-1} + \mathbf{C}_{il}^{-1} \mathbf{C}_{kj}^{-1}), \quad i, j, k, l = 1, 2, 3. \quad (3.26)$$

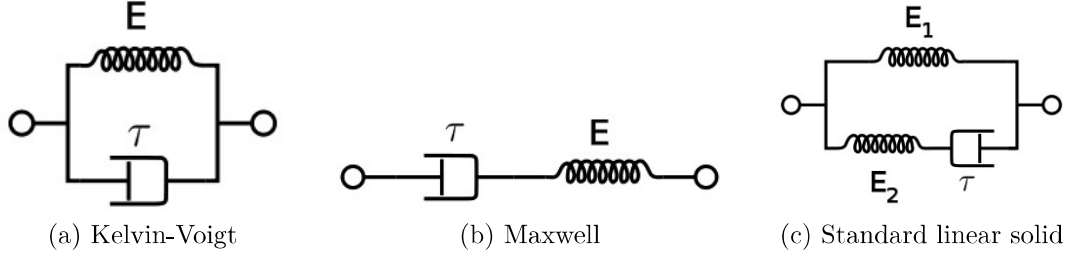


Figure 3.2: Spring-dashpot models for linear viscoelastic material behavior (source: wikipedia.org). E resp. E_1 and E_2 are the stiffnesses of linear springs and τ is the relaxation time of a damper element

3.1.4 Visco-hyperelasticity

While the static or quasi-static behavior of materials such as rubber or elastomers can be described by (almost incompressible) hyperelastic materials laws, they show viscoelastic, time- resp. frequency- (and temperature-) dependent material properties when subject to harmonic loading [25, 46, 78, 130].

In one dimension several rheological models, i.e. spring-dashpot constitutive models, exist for describing viscoelastic behavior and among them are (see also Figure 3.2):

- Kelvin-Voigt:

$$\sigma = E\varepsilon + \tau\dot{\varepsilon} \quad (3.27)$$

- Maxwell:

$$E\sigma + \tau\dot{\sigma} = E\tau\dot{\varepsilon} \quad (3.28)$$

- Standard linear solid / generalized Maxwell:

$$E_2\sigma + \tau\dot{\sigma} = E_1E_2\varepsilon + (E_1 + E_2)\tau\dot{\varepsilon} \quad (3.29)$$

Here τ is called *relaxation time* and $\eta = \tau/E = \tan(\delta)$ is the *loss factor*.

We extend 3-dimensional hyperelasticity to time-dependent visco-hyperelasticity by the following enhancement of the PK2 stress tensor based on the Kelvin-Voigt model [46, 130]:

$$\mathbf{S} = \mathbf{S}_e + \mathbf{S}_v. \quad (3.30)$$

Here, \mathbf{S}_e represents the hyperelastic stress contribution and \mathbf{S}_v the viscous stress contribution, which depends on the rate of the Green-Lagrange strain $\dot{\mathbf{E}}$. \mathbf{S}_e is selected from one of the hyperelastic constitutive laws and possible examples for \mathbf{S}_v are

$$\mathbf{S}_v = 2\eta\mu\dot{\mathbf{E}}. \quad (3.31)$$

in analogy to linear viscoelasticity, or from [130]:

$$\mathbf{S}_v = J\tau\mathbf{C}^{-1}\dot{\mathbf{E}}\mathbf{C}^{-1}. \quad (3.32)$$

In harmonic motion the material parameters such as Young's modulus E , loss factor η and eventually Poisson's ratio ν are typically not constant, but depend on the frequency f resp. angular frequency $\omega = 2\pi f$. An example for a material with strongly frequency-

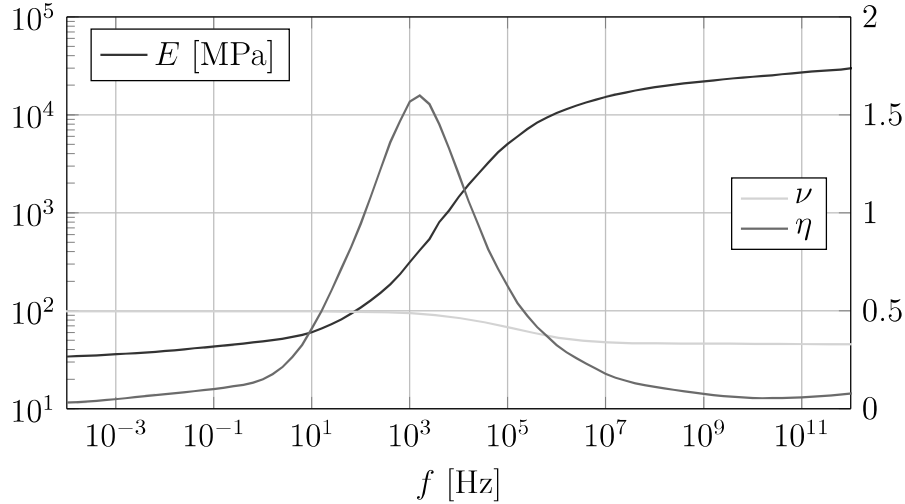


Figure 3.3: Example of frequency-dependent material properties: Young's modulus E , Poisson's ratio ν and loss factor η over excitation frequency f for polymer material Viton® 50°ShA

dependent material properties is Viton® 50°ShA, a polymer which is frequently used for sealing rings and gaskets. Measurements of material properties have been obtained at Siemens and are shown in Figure 3.3.

However, realistic modeling of materials with viscoelastic properties in general is a wide field of scientific research by itself and thus beyond the scope of this work. As material properties are very characteristic for a specific material used, we take the frequency-dependent properties of Viton® 50°ShA, as given in Figure 3.3, as an example to test the methods developed in this thesis.

3.2 Nonlinear isogeometric finite element analysis

Since an analytical solution of problems in nonlinear mechanics is usually not possible for complicated domains and material laws, we seek a numerical approximation using an isogeometric finite element discretization of continuum mechanics equations. It is based on the weak form of the equation of motion (Section 3.2.1) and isogeometric spline discretizations of geometry and displacement field (Section 3.2.2). The resulting nonlinear system of equations, which needs to be solved in order to determine the unknown control point displacements of a static deformation, is solved by a Newton's method (Section 3.2.3).

3.2.1 Weak form of the equation of motion

To find an approximate solution \mathbf{u}^h of the exact displacement \mathbf{u} of the nonlinear continuum mechanics problem governed by balance equations introduced in Section 3.1.2, we only demand that the equation of motion (3.11) is fulfilled in a weak sense [130]. Thus the residual remaining from (3.11) is multiplied with a test function $\delta\mathbf{u}$, the so-called virtual displacement fulfilling the boundary condition $\delta\mathbf{u} = \mathbf{0}$ on Γ_u , and then integrated over

the domain Ω :

$$\int_{\Omega} \left\{ \rho_0 \delta \mathbf{u}^T \ddot{\mathbf{u}}^h - \delta \mathbf{u}^T \operatorname{div} \left(\mathbf{F}(\mathbf{u}^h) \mathbf{S}(\mathbf{u}^h) \right) - \rho_0 \delta \mathbf{u}^T \mathbf{b} \right\} d\mathbf{x} = 0 \quad \forall \delta \mathbf{u}. \quad (3.33)$$

Integration by parts of this *principle of virtual work* and application of divergence theorem yield:

$$\int_{\Omega} \rho_0 \delta \mathbf{u}^T \ddot{\mathbf{u}}^h d\mathbf{x} + \int_{\Omega} \nabla(\delta \mathbf{u}) \cdot \left(\mathbf{F}(\mathbf{u}^h) \mathbf{S}(\mathbf{u}^h) \right) d\mathbf{x} = \int_{\Omega} \rho_0 \delta \mathbf{u}^T \mathbf{b} d\mathbf{x} + \int_{\Gamma_n} \delta \mathbf{u}^T \mathbf{t} d\Gamma. \quad (3.34)$$

This can be rewritten using the variation of the Green-Lagrange strain tensor

$$\delta \mathbf{E} = \frac{1}{2} \left(\nabla(\delta \mathbf{u})^T \mathbf{F} + \mathbf{F}^T \nabla(\delta \mathbf{u}) \right) \quad (3.35)$$

as the weak form of the equation of motion:

$$\int_{\Omega} \rho_0 \delta \mathbf{u}^T \ddot{\mathbf{u}}^h d\mathbf{x} + \int_{\Omega} \delta \mathbf{E} \cdot \mathbf{S}(\mathbf{u}^h) d\mathbf{x} = \int_{\Omega} \rho_0 \delta \mathbf{u}^T \mathbf{b} d\mathbf{x} + \int_{\Gamma_n} \delta \mathbf{u}^T \mathbf{t} d\Gamma \quad \forall \delta \mathbf{u}. \quad (3.36)$$

The first term on the left of the equality sign refers to the virtual change in kinetic energy, the second to the internal virtual work and the terms on the right to the external virtual work from applied body forces and surface tractions.

In the case of compressible hyperelastic materials, a displacement-based strain energy function ψ exists, describing the elastic energy stored in the solid. Then the *virtual work equation* (3.36) of the static problem, where $\ddot{\mathbf{u}} = \mathbf{0}$, can also be derived by minimizing an elastic energy functional [7, 130]:

$$\Pi_d(\mathbf{u}) = \int_{\Omega} \psi(\mathbf{C}) d\mathbf{x} - \int_{\Omega} \rho_0 \mathbf{b} d\mathbf{x} + \int_{\Gamma_n} \mathbf{t} d\Gamma \rightarrow \min. \quad (3.37)$$

An approximation of the minimizer \mathbf{u}^h can then be found by setting the first variation of (3.37) to zero, i.e. $d\Pi_d(\mathbf{u}^h)[\delta \mathbf{u}] = 0$, which leads to the virtual work equation (3.36) (without the kinetic energy term).

3.2.2 Isogeometric finite element discretization

For the spatial discretization and solution of the virtual work equation (3.36) we use the isogeometric finite element method as introduced in Section 2.2.1.

Starting point is a trivariate spline volume parameterization of material coordinates, i.e. the geometry function mapping a parameter domain $\Omega_0 \subset \mathbb{R}^3$ onto the material coordinates $\mathbf{x} \in \Omega \subset \mathbb{R}^3$:

$$\mathbf{x} = \mathbf{g}(\boldsymbol{\xi}) = \sum_{i=1}^n N_i^p(\boldsymbol{\xi}) \mathbf{v}_i, \quad \boldsymbol{\xi} \in \Omega_0. \quad (3.38)$$

As already mentioned in Section 2.1.2, degree p , number of basis functions n and index i should be understood as 3-dimensional vectors resp. multi-indices.

The discretized spaces for displacements $\mathbf{u}^h \in \mathcal{S}^h \subset \mathcal{S}$ and virtual displacements $\delta \mathbf{u}^h \in \mathcal{V}^h \subset \mathcal{V}$ are selected as push-forward of the spline spaces defining the geometry onto the material coordinates, see (2.10):

$$\begin{aligned}\mathbf{u}^h(\mathbf{x}, t) &= \sum_{i=1}^n N_i^p(\mathbf{g}^{-1}(\mathbf{x})) \mathbf{d}_i(t), \\ \delta \mathbf{u}^h(\mathbf{x}) &= \sum_{i=1}^n N_i^p(\mathbf{g}^{-1}(\mathbf{x})) \delta \mathbf{d}_i.\end{aligned}\tag{3.39}$$

The kinematic quantities described in Section 3.1.1 have to be evaluated depending on the discretized displacements. For the deformation gradient this means:

$$\begin{aligned}\mathbf{F}(\mathbf{x}, t) &= \mathbf{I} + \nabla \mathbf{u}^h(\mathbf{x}, t) = \mathbf{I} + \sum_{i=1}^n \mathbf{d}_i(t) \nabla N_i^p(\mathbf{x}) \\ &= \mathbf{I} + \sum_{i=1}^n \mathbf{d}_i(t) \frac{dN_i^p}{d\xi}(\mathbf{g}^{-1}(\mathbf{x})) \cdot \left(\frac{d\mathbf{g}}{d\xi} \right)^{-1}.\end{aligned}\tag{3.40}$$

Cauchy-Green and Green-Lagrange strain tensors can then be computed from \mathbf{F} and the 2nd Piola-Kirchhoff stress can be evaluated. Switching to the Voigt vector notation for matrices \mathbf{E} and \mathbf{S} (see [130])

$$\begin{aligned}\vec{\mathbf{E}} &= (E_{11}, E_{22}, E_{33}, 2E_{12}, 2E_{23}, 2E_{13})^T, \\ \vec{\mathbf{S}} &= (S_{11}, S_{22}, S_{33}, S_{12}, S_{23}, S_{13})^T,\end{aligned}\tag{3.41}$$

the virtual Green-Lagrange strain tensor can be written as

$$\delta \vec{\mathbf{E}}_i(\mathbf{x}) = \mathbf{B}_i(\mathbf{x}) \delta \mathbf{d}_i,\tag{3.42}$$

with virtual displacement control points $\delta \mathbf{d}_i$ and the matrix $\mathbf{B}_i \in \mathbb{R}^{6 \times 3}$ as:

$$\begin{aligned}\mathbf{B}_i(\mathbf{x}) &= \begin{pmatrix} F_{11}N_{i,1}^p & F_{21}N_{i,1}^p & F_{31}N_{i,1}^p \\ F_{12}N_{i,2}^p & F_{22}N_{i,2}^p & F_{32}N_{i,2}^p \\ F_{13}N_{i,3}^p & F_{23}N_{i,3}^p & F_{33}N_{i,3}^p \\ F_{11}N_{i,2}^p + F_{12}N_{i,1}^p & F_{21}N_{i,2}^p + F_{22}N_{i,1}^p & F_{31}N_{i,2}^p + F_{32}N_{i,1}^p \\ F_{12}N_{i,3}^p + F_{13}N_{i,2}^p & F_{22}N_{i,3}^p + F_{23}N_{i,2}^p & F_{32}N_{i,3}^p + F_{33}N_{i,2}^p \\ F_{11}N_{i,3}^p + F_{13}N_{i,1}^p & F_{21}N_{i,3}^p + F_{23}N_{i,1}^p & F_{31}N_{i,3}^p + F_{33}N_{i,1}^p \end{pmatrix} \\ &\triangleq \frac{1}{2} \left(\nabla N_i^p(\mathbf{x})^T \mathbf{F}(\mathbf{x}) + \mathbf{F}(\mathbf{x})^T \nabla N_i^p(\mathbf{x}) \right).\end{aligned}\tag{3.43}$$

Inserting all the discretized kinematic quantities into the weak form of the equation of motion (3.36) then yields:

$$\begin{aligned}\delta \mathbf{d}_i^T \int_{\Omega} \rho_0 N_i^p \mathbf{I} N_j^p d\mathbf{x} \ddot{\mathbf{d}}_j &+ \delta \mathbf{d}_i^T \int_{\Omega} \mathbf{B}_i^T \vec{\mathbf{S}}(\mathbf{d}) d\mathbf{x} \\ &= \delta \mathbf{d}_i^T \int_{\Omega} \rho_0 N_i^p \mathbf{b} d\mathbf{x} + \delta \mathbf{d}_i^T \int_{\Gamma_n} N_i^p \mathbf{t} d\Gamma \quad i, j = 1, \dots, n.\end{aligned}\tag{3.44}$$

Since this equation has to be fulfilled for all admissible $\delta \mathbf{d}_i$, we finally arrive at the

discretized equation of motion, just as in standard finite element methods [62, 130]:

$$\mathbf{M} \ddot{\mathbf{d}}(t) + \mathbf{f}(\mathbf{d}(t)) = \mathbf{b}(t), \quad (3.45)$$

which needs to be solved for the unknown vector of control point displacements \mathbf{d} . Therefore the entries of the *internal force vector* $\mathbf{f} \in \mathbb{R}^N$,

$$\mathbf{f}_i = \int_{\Omega} \mathbf{B}_i^T \vec{\mathbf{S}}(\mathbf{d}) d\mathbf{x} \quad i = 1, \dots, n, \quad (3.46)$$

the *external force vector* $\mathbf{b} \in \mathbb{R}^N$,

$$\mathbf{b}_i = \int_{\Omega} \rho_0 N_i^p \mathbf{b} d\mathbf{x} + \int_{\Gamma_n} N_i^p \mathbf{t} d\Gamma \quad i = 1, \dots, n, \quad (3.47)$$

and the consistent *mass matrix* $\mathbf{M} \in \mathbb{R}^{N \times N}$,

$$\mathbf{M}_{ij} = \mathbf{I} \int_{\Omega} \rho_0 N_i^p N_j^p d\mathbf{x} \quad i, j = 1, \dots, n, \quad (3.48)$$

have to be assembled.

3.2.3 Solution of the static problem

In the elastostatic problem the time-dependence of external force and internal variables is neglected and the equation of motion (3.11) is

$$-\operatorname{div} \mathbf{F} \mathbf{S}(\mathbf{u}) = \rho_0 \mathbf{b}, \quad (3.49)$$

and its discretized form, compare (3.45), reads:

$$\mathbf{f}(\mathbf{d}) = \mathbf{b}. \quad (3.50)$$

Existence of a solution

As in detail discussed in [35, 83], a number of constitutive assumptions has to be made in order to show the existence of a solution of the continuous problem of elasticity (3.49). These include:

- Isotropy and the existence of a stored energy function ψ , see Section 3.1.3
- For small strains the stored energy function must take the form

$$\psi(\mathbf{E}) = \frac{\lambda}{2} \operatorname{tr}(\mathbf{E})^2 + \mu \operatorname{tr}(\mathbf{E}^2) + \mathcal{O}(\|\mathbf{E}\|^2) \quad (3.51)$$

- Large strains must result in large stresses, i.e.

$$\lim_{\det \mathbf{F} \rightarrow +0} \psi(\mathbf{F}) = +\infty \quad \wedge \quad \lim_{\det \mathbf{F} \rightarrow +\infty} \psi(\mathbf{F}) = +\infty \quad (3.52)$$

- Poly- or quasi-convexity of the strain energy function

Algorithm 1 Newton's method for nonlinear elasticity

```

1: Initial guess:  $\mathbf{d}^0$ 
2: Tolerances:  $\varepsilon_d, \varepsilon_r > 0$ 
3: Initialization:  $s \leftarrow 0$ 
4: repeat
5:   Assembly:  $\mathbf{f}^s \leftarrow \mathbf{f}(\mathbf{d}^s), \mathbf{K}_T^s \leftarrow \mathbf{K}_T(\mathbf{d}^s)$ 
6:   Evaluate residual:  $\mathbf{r}^s \leftarrow \mathbf{f}^s - \mathbf{b}$ 
7:   Compute update:  $\Delta \mathbf{d}^s \leftarrow \text{Solve } \mathbf{K}_T^s \Delta \mathbf{d}^s = -\mathbf{r}^s$ 
8:   Evaluate error:  $e_d \leftarrow \frac{\|\Delta \mathbf{d}^s\|}{\|\mathbf{d}^s\|}, e_r \leftarrow \frac{\|\mathbf{r}^s\|}{\|\mathbf{b}\|}$ 
9:   Update:  $\mathbf{d}^{s+1} \leftarrow \mathbf{d}^s + \Delta \mathbf{d}^s$ 
10:   $s \leftarrow s + 1$ 
11: until  $e_d < \varepsilon_d \wedge e_r < \varepsilon_r$ 
12: Return value:  $\mathbf{d} \leftarrow \mathbf{d}^s$ 
    
```

- The Legendre-Hadamard condition, i.e. ellipticity or positive definiteness of the elasticity tensor $\mathbb{C}(\mathbf{F})$ (3.24)

Under these constitutive and further assumptions, such as smoothness of the boundary of Ω , it is shown in [35, 83] that a nonlinear elasticity problem has a solution in the neighborhood of the solution of the linearized problem (Section 3.3). However, in practical applications some of these conditions might be violated and in general several (or even infinite) solutions may exist and bifurcation of solution paths can occur.

Numerical solution using Newton's method

To solve the nonlinear system of equations (3.50) for the unknown control point displacements \mathbf{d} , it is rewritten in residual form:

$$\mathbf{r}(\mathbf{d}) = \mathbf{f}(\mathbf{d}) - \mathbf{b} = \mathbf{0}. \quad (3.53)$$

Typically, iterative procedures are used to find an approximate solution of the residual equation, such as fixed-point methods, Newton-Raphson methods, modified or quasi-Newton methods, and arc-length continuation methods [130].

In Algorithm 1 we describe the use of a classical Newton-Raphson method for the solution of the static nonlinear elasticity problem (3.53).

As initial guess typically $\mathbf{d}^0 = \mathbf{0}$ is used, which yields the solution of the linear problem as \mathbf{d}^1 in the first iteration. In case Algorithm 1 is part of a loop with increasing load factor $\lambda = 1, 2, \dots$ for the right-hand side $\mathbf{b}(\lambda) = \lambda \mathbf{b}$, the result of the previous load step is used. Since the solution of (3.50) is not necessarily unique and Newton's method can only find a solution in the neighborhood of the initial guess, \mathbf{d}^0 is a crucial input quantity.

The matrix $\mathbf{K}_T(\mathbf{d})$ is the so-called *tangential stiffness matrix*. It is the derivative of the residual \mathbf{r} , resp. the internal force vector \mathbf{f} , w.r.t. the displacement vector \mathbf{d} :

$$\mathbf{K}_T(\mathbf{d}) = \frac{d\mathbf{r}}{d\mathbf{d}}(\mathbf{d}) = \frac{d\mathbf{f}}{d\mathbf{d}}(\mathbf{d}). \quad (3.54)$$

It can be computed and assembled as a sum of two matrices:

$$\mathbf{K}(\mathbf{d}) = \mathbf{K}^{geo}(\mathbf{d}) + \mathbf{K}^{mat}(\mathbf{d}), \quad (3.55)$$

with the geometric tangent matrix

$$\mathbf{K}_{ij}^{geo}(\mathbf{d}) = \sum_{e=1}^{\ell} \left\{ \mathbf{I} \int_{\Omega_e} \nabla N_i^p{}^T \mathbf{S}(\mathbf{d}) \nabla N_j^p dx \right\} \quad (3.56)$$

and the material tangent matrix

$$\mathbf{K}_{ij}^{mat}(\mathbf{d}) = \sum_{e=1}^{\ell} \left\{ \int_{\Omega_e} \mathbf{B}_i^T \mathbb{C}(\mathbf{d}) \mathbf{B}_j dx \right\}. \quad (3.57)$$

Here $\mathbb{C} = \frac{d\mathbf{S}}{d\mathbf{E}} \in \mathbb{R}^{6 \times 6}$ is the matrix form of the constitutive 4th order tensor (3.24).

The internal force vector \mathbf{f}^s and tangential stiffness matrix \mathbf{K}_T^s have to be reassembled in every step s of the iteration, since they depend on the current displacement \mathbf{d}^s , while the right-hand side vector \mathbf{b} stays constant, as we do not consider right-hand sides dependent on \mathbf{d} .

The structure and solution procedure of the system $\mathbf{K}_T^s \Delta \mathbf{d}^s = -\mathbf{r}^s$ for the displacement update $\Delta \mathbf{d}^s$ is also completely analogous to the general linear case, see Sections 2.2.2.

Two convergence criteria are checked: e_d is measuring the relative size of the increment in the s -th step and e_r is the norm of the residual, normalized by the norm of the right-hand side. Once the convergence criteria are met, the displacement from the last iteration step \mathbf{d}^s is returned and can be used to compute the current configuration $\mathbf{y} = \mathbf{x} + \mathbf{u}(\mathbf{x})$ as displaced NURBS volume and other postprocessing results such as evaluation of stresses and strains.

Remark 3.1. *As discussed for general linear problems in Section 2.3, an extension of the isogeometric finite element discretization of nonlinear elasticity to multi-patch parameterizations is possible in a straight-forward manner. It was also implemented for the numerical examples discussed in this thesis.*

3.3 Brief note on linear elasticity

Linear elasticity theory can be interpreted as a linearization of nonlinear theory around the undeformed and stress-free initial state [83]. It is only valid for small displacements and strains, i.e. when $\|\nabla \mathbf{u}\| \ll 1$. Here we briefly review the equations and IGA discretization of linear elasticity, since we are going to compare results of linear and nonlinear analysis for validation of methods and implementations, for instance in Section 3.5.

The equation of motion of linear elasticity, compare (3.11), reads

$$\rho \ddot{\mathbf{u}} - \operatorname{div} \boldsymbol{\sigma}(\mathbf{u}) = \rho \mathbf{b}, \quad (3.58)$$

where the Cauchy stress $\boldsymbol{\sigma}$ is expressed by the linear St. Venant-Kirchhoff constitutive